Land surface temperature predicts mortality due to chronic obstructive pulmonary disease: a study based on climate variables and impact machine learning

Alireza Mohammadi,[1] Bardia Mashhoodi,[2] Ali Shamsoddini,[3] Elahe Pishgar,[4] Robert Bergquist[5]

[1]Department of Geography and Urban Planning, Faculty of Social Sciences, University of Mohaghegh Ardabili, Ardabil, Iran; [2]Landscape Architecture and Spatial Planning Group, Department of Environmental Sciences, Wageningen University & Research, Wageningen, Netherlands; [3]Department of Architecture and Urban Planning, Shiraz Branch, Islamic Azad University, Shiraz, Iran; [4]Human Geography and Spatial Planning, Faculty of Earth Science, Shahid Beheshti University, Tehran, Iran; [5]Ingerod, Brastad, Sweden

Correspondence: Alireza Mohammadi, Department of Geography and Urban Planning, Faculty of Social Sciences, University of Mohaghegh Ardabili, Ardabil, Iran.
Tel.: +989126844392
E-mail: alirezamohammadi20142014@gmail.com

Key words: chronic obstructive pulmonary disease, spatial correlation, predictive modelling, forest-based classification and regression model, geographic information systems, remote sensing data, United States.

Contributions: AM, conceptualization, methodology/study design, software, validation, formal analysis, writing – original draft, visualization, supervision, funding acquisition; BM, writing – original draft, writing – review and editing; AS, data curation, visualization; EP, data curation, visualization; RB, writing - review and editing. All authors contributed to the article and approved the submitted version.

Conflict of interest: the authors declare no potential conflict of interest, and all authors confirm accuracy.

Availability of data and materials: the deaths from Chronic Obstructive Pulmonary Disease (COPD) data that support the findings of this study are available from: https://ephtracking.cdc.gov/DataExplorer

Conflict of interest: the authors declare that there is no conflict of interest.

Funding: this study received financial support from the University of Mohaghegh Ardabili (#19308).

Acknowledgements: this work is supported by the University of Mohaghegh Ardabili. So, the authors are grateful to the Director of University of Mohaghegh Ardabili. We also thank the United States Centers for Disease Control and Prevention (CDC) for providing us with the COPD related spatial data.

Received: 9 June 2024.
Accepted: 23 December 2024.

Geospatial Health 2025; 20:1319
doi:10.4081/gh.2025.1319

Abstract

Chronic Obstructive Pulmonary Disease (COPD) has been the focus of scientists and policymakers in the past decade with regard to mortality rates and global warming. The long-term shift in temperature and weather patterns, commonly called climate change, is an important public health issue, especially concerning COPD. Using the most recent county-level age-adjusted COPD mortality rates among adults older than 25 years, this study aimed to investigate the spatial trajectory of COPD in the United States between 2001 and 2020. Global Moran's *I* was used to investigate spatial relationships utilising data from Terra satellite for night-time Land Surface Temperatures (LST_{nt}), which served as an indicator of warming within the same time period across the United States. The Forest-based Classification and Regression model (FCR) was applied to predict mortality rates. It was found that COPD mortality over the study period was spatially clustered in certain counties. Moran's *I* statistic (0.18) showed that the COPD mortality rates increased with LST_{nt}, with the strongest spatial association in the eastern and south-eastern counties. The FCR model successfully predicted mortality rates in the study area using LST_{nt} values, achieving an R^2 value of 0.68, which accounted for COPD mortality rates independently. Policymakers in the United States could use the findings of this study to develop long-term spatial and health-related strategies to reduce the vulnerability to global warming of patients with acute respiratory symptoms.

Introduction

Chronic Obstructive Pulmonary Disease (COPD) is a heterogeneous lung condition characterized by chronic respiratory symptoms (dyspnoea, cough, sputum production and/or exacerbations) due to airway abnormalities (bronchitis, bronchiolitis) and/or alveolar injury (emphysema) that cause persistent, often progressive airflow obstruction (Celli *et al*., 2022; Htwe *et al.*, 2023) It is a not fully reversible disorder characterized by progressive airflow limitation associated with an abnormal inflammatory response of the lungs to noxious particles or gases (Bracke & Brusselle, 2015). According to the World Health Organization (WHO), the most common symptoms are difficult breathing, chronic cough (sometimes with phlegm) and a feeling of tiredness, symptoms that can quickly get worse (WHO, 2023a). People with COPD are also exposed to a higher risk of other health problems, such as respiratory infections, heart problems, lung cancer and lung arterial hypertension (WHO, 2023a), which often lead to depression and sometimes mental health setbacks (Hurst et al. 2020). By causing more than 3.3 million deaths worldwide (WHO, 2023b), and increasing in prevalence (Cushen, Morgan, & Summer 2017; Tourre *et al.*, 2022), COPD is now the third leading cause of death worldwide. Indeed, COPD affects more than 15 million Americans and accounts for most of the deaths from chronic lower respiratory diseases, which in 2020 was the sixth leading cause of death in the United States (U.S.). According to the Centers for Disease Control and Prevention (CDC) in the U.S., more than 150,000 Americans die from COPD each year – that is 1 death every 4 minutes (CDC, 2023). Although this disease is almost completely preventable, it still poses a public health threat.

COPD exacerbations can be triggered by increased dyspnoea, reduced lung function, poorer quality of life, and prior exacerbations; comorbidities, *e.g.*, cardiovascular events, depression and a history of gastroesophageal reflux or heartburn. In addition, it can be elicited by demographic characteristics, such as sex and age and is often associated with biomarkers, *e.g*., elevated white blood cell counts (Hurst *et al.*, 2020). According to previous studies, people aged 65 years or older (men in general), habitual tobacco smokers and people with a history of asthma are more likely to die from COPD (American Lung Association, 2023; CDC, 2023). Several of these and other previous studies have reported outdoor air pollution as a major risk factor, which is estimated to cause 43% of all COPD deaths (Hansel *et al.*, 2016; Sama *et al.*, 2017; WHO, 2023b; CDC, 2023). For example, a study in China showed that increased concentrations of airborne pollutants composed of particular matter less than 2.5 µm ($PM_{2.5}$) and chemical elements, such as SO_2, NO_2, O_3 and CO are significantly and positively associated with COPD mortality rates (Chen *et al.*, 2021).

The long-term shifts in temperature and weather patterns (Lovejoy, 2013), commonly referred to as Climate Change, is an important public health issue, especially with regard to diseases affecting the respiratory system (Tran *et al.*, 2022). Since 1901, the average surface temperature across the contiguous U.S. has risen at an average rate of 0.17°F (0.09°C) per decade and the years 2012, 2016 and 2020 were among the warmest years of the last decades (National Centers for Environmental Information, 2023). Higher mean temperatures are recorded each year, and more people are being affected by climate-sensitive diseases as well as natural disasters caused by climate change. Approximately 250,000 deaths per year are expected to occur over the next few decades in response to more frequent extreme weather events (Mertes *et al.*, 2021). Indeed, many studies set Climate Change as an important risk factor for COPD-associated exacerbation and mortality (Hess *et al.*, 2009; D'Amato *et al.*, 2014; Sama *et al.*, 2017; de Miguel-Díez *et al.*, 2019; Duan *et al.*, 2020; Ozturk *et al.*, 2023). Among climatological factors, precipitation, humidity and wind are directly related to the temperature variations both in the short and the long term (Subramanian *et al.*, 2023). Human activities have been the main driver of Climate Change, primarily due to burning fossil fuels like coal, oil and gas that produce CO_2 blocking heat radiation from Earth into space (Mertes *et al.*, 2021), a fact that increases the problem in settlements where current populations are exposed to severe health-related threats (Duvat *et al.*, 2021).

Environmental factors such as Climate Change have long been associated with chronic respiratory diseases (Shiau *et al.*, 2023) and these consequences are linked to serious health risks, particularly for vulnerable groups like the elderly (Tilstra *et al.*, 2022). The association between temperature variations and COPD mortality has been studied extensively (Hansel *et al.*, 2016; Tian *et al.*, 2021; Fu *et al.*, 2022; Tran *et al.*, 2023). Gu *et al.* (2022), using a quasi-Poisson generalized linear regression model, found that exposure to extreme temperature in Hangzhou City, China was associated with increased COPD mortality, thereby confirming the results by a previous study (Tian *et al.*, 2021) in 21 cities of Guangdong Province, South China, who used a similar approach but based on a distributed lag nonlinear model. Several studies confirm that also colder temperatures are associated with higher COPD mortality (Donaldson *et al.*, 2012; Jenkins *et al.*, 2012; Viggers *et al.*, 2013; McCormack *et al.*, 2017). For example, a study in 6 metropolitan cities in Taiwan concluded that the mortality risk of COPD in elderly men was significantly associated with extremely low temperatures (Zafirah *et al.*, 2021). A study in Weifang City, China, Diao *et al.* (2021) found that the combination of air pollution and low temperature increases the COPD mortality risk. Another study in Taiwan, showed that climate change increased COPD severity and mortality (Chuang *et al.*, 2022). In a study in Jiading District, Shanghai, China, Peng *et al.* (2021), using Geographically Weighted Logistic Regression (GWLR), confirmed that extremely low temperatures increased COPD mortality, while Tran *et al.* (2023) found a negative correlation between COPD mortality and temperatures ranging between 3.8° and 29.9°. Thus, results regarding the impact of low and high temperatures on COPD vary across different geographies (Duan *et al.*, 2020; Sama *et al.*, 2017).

During the last few years, remote sensing data have increasing been used in monitoring, spatial predictive modelling, surveillance, and risk assessment with respect to human health (Alvarez-Mendoza *et al.*, 2020). However, a knowledge gap is evident in the previous studies on COPD mortality: the impact of long-term change of night-time land surface temperatures (LST_{nt}) on COPD mortality remains unclear. Additionally, it is unknown if such impact varies across a large-scale territory. The reason for the use of LST_{nt} is that this satellite-generated variable is a well-established proxy to measure and confirm Climate Change in a specific geographical area. The use of U.S. counties for case study was taken as it represents a very large area, for which long-term reliable data on both LST_{nt} and human cases are available.

In our study, we prioritized the understanding of local relationships between Land Surface Temperature (LST) and COPD mortality rates rather than addressing all well-known risk factors superficially. Analysing LST is crucial as it directly affects heat stress, influences air quality through the formation of pollutants and reflects regional temperature variations, all of which influence respiratory health strongly, especially within the context of Climate Change (Hansel *et al.*, 2016; Fu *et al.*, 2022; He *et al.*, 2022). By narrowing our focus, we aimed to provide a more nuanced analysis of how LST specifically contributes to respiratory health outcomes, allowing us to uncover local variations and interactions that may be overlooked when considering the broader risk. This concentrated approach offers insights essential for developing targeted public health interventions and advancing our understanding of the complex dynamics between climate and health. This study is significant as it investigates the relationship between LST_{nt} and COPD mortality rates, thereby explaining the implications of climate change on public health. Given the increasing frequency of extreme heat events and changing climate patterns, understanding how LST influences respiratory health outcomes is essential for developing effective public health interventions. By isolating the impact of LST, this research aims to inform strategies for mitigating health risks associated with rising temperatures, ultimately contributing to the enhancement of public health resilience in the context of climate change.

This study aimed to i) disclose the general geography of COPD between 2001 and 2020 in the U.S.; ii) measure the spatial correlations between LST_{nt} and COPD mortality rates; iii) develop a COPD mortality prediction model based on LST_{nt}; and iv) identify high-risk areas.

Materials and Methods

Data

Geospatial data

County-level population data including geographic boundaries of the contiguous states were acquired from the U.S. Census Bureau (United States Census Bureau 2022). The EPSG:4326 - WGS 84 projection system was used for projecting all the formats of Geographical Information Systems (GIS) layers of the study area based on World Geodetic System 1984 ensemble. We used this projection system because the contiguous U.S. ranges from approximately 24.52N to 49.38N latitude and 66.95W to 124.77 W longitude (Geodatos 2023).

COPD mortality data

The COPD mortality rate for the period 2001-2020 among the population ≥25 years old was used as the dependent variable. The reason for the choice of the data for this age group is that that over 99% COPD in the U.S. occurs in this age group. In 2020, for example, the rate of COPD mortality was substantially higher among older age groups (CDC, 2023). The U.S. CDC provides county-level, age-adjusted death rate from COPD among ≥25 years olds for the years 2001-2020 (CDC, 2023). Death from COPD in this presentation was defined based on codes from the tenth revision of International Classification of Diseases (ICD-10), *i.e.*, chronic bronchitis (J40-42), emphysema (J43) and other chronic obstructive pulmonary disease (J44). Rates were age-adjusted by direct methods using the U.S. Standard Population for the year 2000, a measure that can was also used to assess mortality trends over time and identify high–risk populations by area (CDC, 2023).

To ensure the quality and reliability of the COPD and geospatial data in this study, we obtained county-level population and COPD mortality data from trusted organizations, specifically the U.S. Census Bureau and CDC. The former follows strict statistical quality standards during data collection and reporting, covering planning, collection, processing, and dissemination stages to uphold high data integrity. Similarly, the CDC implements rigorous data management protocols to ensure the reliability of its health statistics, which are vital for public health planning and intervention. Utilizing data from these authoritative sources bolsters the credibility of our findings and contributes to a robust evidence base for understanding COPD trends and their implications for public health.

LST_{nt} data

The 8-Day global package of the moderate resolution imaging spectroradiometer (MODIS)'s LST/Emissivity (MOD11A2, version 6.1) generated by the Terra and Aqua satellites was extracted from the National Aeronautics and Space Administration (NASA)'s remote sensing data collection of the land processes distributed active archive center (LP DAAC) at the U.S. Geological Survey (USGS) EROS Center using the Google Earth Engine (GEE) platform (NASA LP DAAC and DAAC 2023). This package provides an average 8-day, per-pixel LST and emissivity with a 1.2-km spatial resolution (giving a 1.2 by 1.2 km grid). Each pixel value in the MOD11A2 is a simple average of all the corresponding MOD11A1 LST pixels collected by the two ground track repeat periods of the Terra and Aqua satellites within each 8-day period. The quality control assessments, observation times, zenith view angles, clear-sky coverage and emissivity data are provided together with the LST_{nt} data (Wan, Hook, & Hulley, 2021). The contagious U.S. area covers 8,080,47 km^2, 3% of which classified as urban and home to 83% of the total population (Center for Sustainable Systems 2019). At night-time, rural areas show lower temperatures than the built-up (urbanized) areas (Bounoua *et al.*, 2017). However, excessive solar radiation during the day can corrupt LST readings since the presence of vegetation has a significant impact on the local surface temperature (Rasul, Balzter, & Smith, 2016). A more reliable indicator for comparing different national areas at the macro scale is therefore provided by LST measurement of night-time, urban heat islands (Bala, Prasad, & Yadav 2020). To carry out the desired analysis, all LST_{nt} values were collected for county polygons. The quality and reliability of the MODIS Land MOD11A2 product are maintained through several built-in quality control measures. NASA's LP DAAC provides bit-encoded Quality Control (QC) layers, which offer detailed information on the conditions under which the data were recorded, such as cloud cover and atmospheric interference. If specific conditions like cloud effects are detected, the LST data are not produced to avoid unreliable readings. Additionally, the mandatory Quality Assurance (QA) flags indicate whether data for certain pixels are valid. The combination of these protocols ensures that the dataset remains highly accurate and reliable for scientific and environmental applications, particularly for measuring surface temperatures under diverse atmospheric conditions.

Analysis and modelling approaches

Mapping the COPD mortality rates

Choropleth maps were used to map COPD mortality rates as well as the LST_{nt} trends using equal intervals and equal counts (quantiles) for the mapping that was based on the Open-Source GIS Platform (QGIS), v. 3.30.3 as described by the QGIS development team 2016) and ArcGIS Pro, v.3.1 (ESRI, Redlands, CA, USA). The Getis-Ord Gi* statistic (Anselin *et al.*, 2009; ESRI, 2010) was utilized to identify the hotspots in the study area and time. Among the different methods of spatial conceptualization relationships for Getis-Ord Gi*, we applied the Contiguity Edges Corners (CEC) approach when calculating all geographical relationships as it is the most appropriate and effective for polygonal features.

Spatial autocorrelation

In this study, LST_{nt} was our exploratory variable. Spatial autocorrelation is the correlation between values of a single variable across a spatial unit (Griffith, 2009). Among the various methods for measuring this correlation, global methods are more sensitive to departures from the null hypothesis (random distribution) (Anselin *et al.*, 2009). For the detection of the spatial autocorrelation of COPD mortality rates for the entire study area and time, we used the R version 4.3.1 software for the application of Global Moran's *I* (GMI), which is generally more accurate regarding measuring autocorrelation than other statistics.

The GMI is a statistical measure used to assess the degree of spatial autocorrelation in a dataset, indicating whether similar values cluster together or disperse across a geographic area. The GMI was employed to quantify spatial autocorrelation, providing insights into the clustering patterns of COPD mortality across the U.S. counties. The GMI was computed according to Anselin *et al.* (2009):

$$I = \frac{n\left(\sum_{i=1}^{n}\sum_{j=1}^{n} w_{ij}\left(x_i - \bar{x}\right)\left(x_j - \bar{x}\right)\right)}{\left(\sum_{i=1}^{n}\sum_{j=1}^{n} w_{ij}\right)\left(\sum_{i=1}^{n}\left(x_i - \bar{x}\right)^2\right)} \quad \text{(Eq. 1)}$$

where n represents the total number of spatial units (*i.e.* U.S. counties); x_i the COPD mortality per 100,000 individuals for county i; $\bar{x}$ the arithmetic mean of the COPD mortality rates; and w_{ij} the spatial weight between counties i and j. The GMI values range between -1 and +1, where values closer to zero indicate non-significant spatial autocorrelation, while values further from zero (either positive or negative) signify strong spatial autocorrelation (Anselin *et al.*, 2009). In this study, the COPD mortality rate was assigned to each county as the value field for analysis. Using spatial analysis tools in ArcGIS software, the GMI was calculated to assess the degree of clustering in the COPD mortality data.

Scatter plots were drawn using the 'ggplot2' package in R to show the correlation between two variables. The main goal of this research was not to study spatiotemporal clusters but to investigate the potential effect of underlying geographic factors. A positive spatial result would pave the way for further studies on possible consequences emanating from such a finding.

Spatial correlation of LST_{nt} and COPD mortality rate

Local Moran's *I* detects clusters of similar values or spatial outliers within a geographic area, as opposed to the overall pattern captured by GMI. In this study, we used the bivariate Local Moran's *I* (shown in Eq. 2) to identify the spatial correlations between COPD mortality rates and the annual mean LST_{nt}. It describes the statistical relationship between one variable at a location and a spatially lagged second variable at neighbouring locations according to Anselin (2020):

$$I_i^{(XY)} = \frac{(x_i - \bar{x})}{\sum_{k=1}^{n}(x_k - \bar{x})^2/(n-1)} \sum_{j=1}^{n} w_{ij}(y_j - \bar{y}) \quad \text{(Eq. 2)}$$

$I_i^{(XY)}$ is the Bivariate Local Moran's I statistic at location i, x_i is $\bar{x}$ is the value of variable X at location i, $\bar{y}$ is the value of variable Y at neighbouring locations j, $\bar{x}$ is the mean of variable X across all locations, $\bar{y}$ is the mean of variable Y across all locations, $\sum_{k=1}^{n}(x_k - \bar{x})^2/(n-1)$ is the variance of variable X and w_{ij} is the spatial weight matrix representing the relationship between location i and its neighbours j, often based on proximity or distance (Anselin 2020; Livings & Wu, 2020)

Bivariate local Moran's *I* can be visualized and mapped using a bivariate Moran scatterplot that displays the relationship between the first variable value at observation *i* and the spatially lagged second variable value at observation *j*, organized into four quadrants (Livings & Wu, 2020). We also mapped the results of bivariate local Moran's *I* result using QGIS.

Prediction based on the FCR model and a ssessment of model performance

Spatial predictions of health variables are of great scientific and societal importance (Wang *et al.*, 2017). There are several spatial prediction models, such as the presence-only prediction (MaxEnt) model (Phillips & Dudík, 2008), the frequency ratio model (Addis, 2023), random forest regression (Joshi, Aliaga, & Teller 2023), spatial statistics model file (ESRI, 2010), logistic and generalized linear regression models (Martínez *et al.*, 2022) to predict a health-related phenomena in a geographical context. Furthermore, even with the most suitable predictive method, it is a challenging to identify and develop the most accurate predictive model(s) (Li, 2019).

In this study, we employed the Forest-based classification and Regression model (FCR) model due to its exceptional ability to manage complex, non-linear relationships and interactions between LST and COPD mortality rates. This model is adept at handling high-dimensional datasets and effectively addresses missing values, which are common in environmental health research (Breiman & Cutler 2014; Friedman, 2001). Additionally, the FCR model provides inherent feature importance metrics, allowing researchers to identify key predictors and gain insights into the impact of climate-related variables on health outcomes (Breiman & Cutler 2014). Utilizing this approach aims to yield robust findings on the influence of LST on COPD mortality while accounting for uncertainties in the data.

The FCR model is a supervised machine-learning method developed by Leo Breiman and Adele Cutler (2014). This model creates models and generates predictions using an adaptation of the random-forest algorithm (ESRI, 2010). First, we tested and selected "predict to features" as our best prediction type. Then, we used the U.S. counties polygon shapefile, which included our variables as input training features. In the next step, we introduced COPD mortality rates as a variable to predict and an annual mean LST_{nt} as our explanatory training variable to the FCR model. The more trees used, the more accurate the model prediction; the number of trees in our FCR model was considered to be 100. Data available per tree (%) was also considered to be 100. For evaluation of the FCR model performance, the training data excluded in the validation was 10%. The number of validations runs required to achieve the highest coefficient of determination, *i.e.*, the squared root (R^2), was set to 5. In the final step, the uncertainty parameter was also considered to measure the prediction interval in FCR model. ArcGIS Pro v.3.1 was utilized to make all predictions. Bivariate choropleth maps, which show the quantitative relation between two variables in a feature layer, were used to represent and compare the FCR model parameter estimates and original values of the explanatory variables. This mapping method is useful for finding the local patterns and variations of two parameters in a single map. The scatterplot with R^2 can also be used to visualize the FCR model performance results. It is a widely used goodness of fit measure (0 to 1 range) for linear regression models to measure the strength of the relationship between the model and the dependent variable on a convenient 0 – 100% scale (Di Mari, Ingrassia, & Punzo 2023). The QGIS and ArcGIS Pro packages were used to visualize our final model results.

Results

Spatiotemporal patterns of the COPD mortality rate

Between the years 2001 and 2020, there were 66,024 confirmed cases of COPD in the U.S. The average rate was 73.9 per 100.000 adults older than 25 years and the Standard Deviation (SD) was 16.8. The highest average rate was recorded for 2008 (78.1) and the lowest for 2004 (69.07). In 2001, the average COPD mortality rate was 71.2 per 100,000, which had dropped to 69.7 per 100,000 in 2020. However, the total period rate, equivalent to 2.7 per 100,000 people, was higher than in 2001. Our analysis showed that males in study time had a higher COPD mortality rate (90.9 per 100,000). Figure 1, shows the spatial distribution of an age-adjusted death rate from COPD per 100.000 population in the 3,108 contiguous U.S. counties using the "equal interval" mode of choropleth mapping. As seen in this map, the COPD mortality rates varied considerably spatiotemporally. For example, some counties of West Virginia and Kentucky have had high mortality rates in most years. Figure 2 shows the average rate range for all the total study period, with rates varying from about 27 to 160 per 100.000. As shown in Figure 2B, the COPD mortality rates vary geographically across the U.S. counties, with hotspots and coldspots, *e,g.*, many Kentucky counties not only experienced high mortality rates but also hotspots. Global Moran's *I* statistic showed a value around 0.85, (SD=79.26, $p<0.001$), with an expected value of 0.00 and a variance of 0.00. The spatial autocorrelation analysis of the 20-year average COPD mortality rates in the study area is illustrated in Figure 2C. The test results indicate that the COPD mortality rates exhibit clustering patterns, with both high and low rates observed. This study examined whether high mortality rates in some counties were possibly associated with changes in LST_{nt}. To discover this correlation, local statistics were applied as the next step.

Spatial distribution and LST_n changes

Figure 3, shows the spatial distribution of the annual mean LST_{nt} values over the study area. These maps show each year's annual mean LST_{nt} values in degrees Celsius for each cell, thus producing high-resolution images (1.2x1,2 km). Based on these spatiotemporal maps, annual average values of LST_{nt} in the study area were seen to vary in a range covering from about -13°C to 27°C. The mean annual LST_{nt} for the study area over the study period was 23, rising from 20.95 in 2001 to 22.0 in 2020. On the

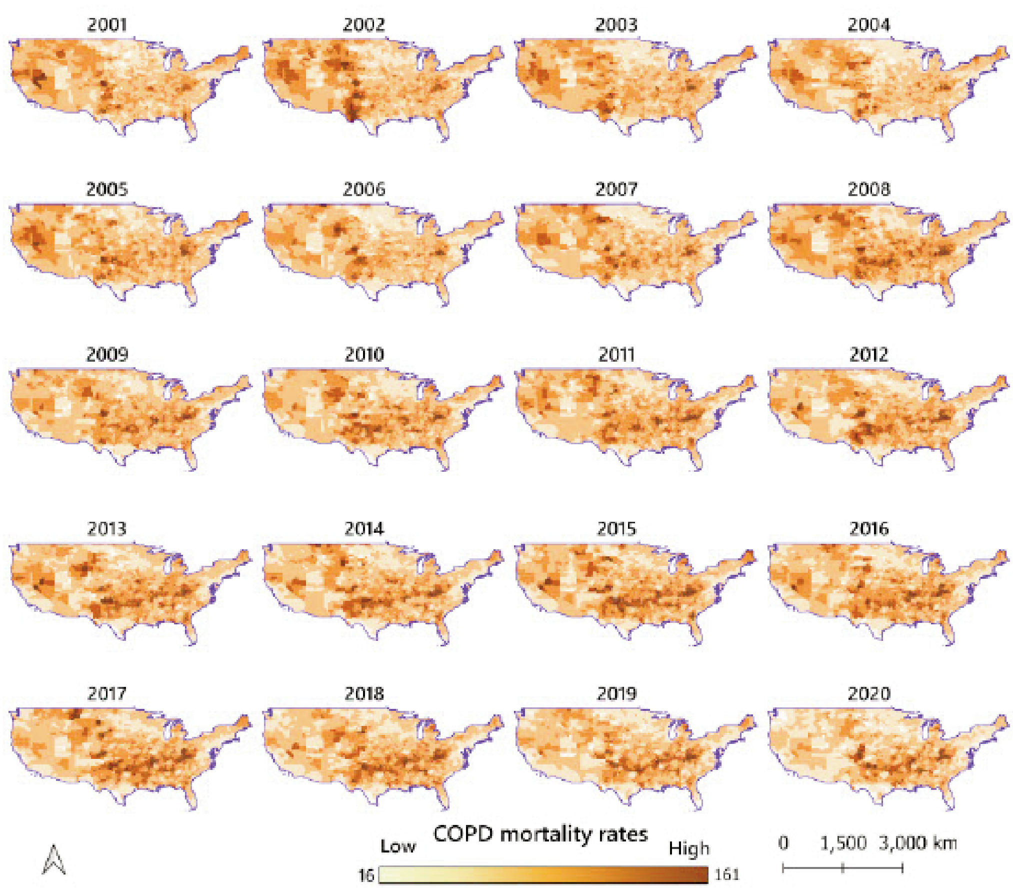

Figure 1. The spatial distribution of the annual average COPD mortality rates (both sexes) per 100.000 population across contiguous United States counties for the period 2001 to 2020.

other hand, however, some years, e.g., 2019, had unusually high mean LST_{nt} values.

Figure 4A depicts the average of the annual mean LST_{nt} values. The results show that the annual mean LST_{nt} values for the entire study area varied from about -11°C to 21.2°C, naturally with the highest mean LSTs (higher than 19 °C) in the South and Southeast. The average LST value calculated per county in 2001 was 7.3°C, a value that had risen to 8.4°C in 2020. Throughout the study period, the average annual LST_{nt} was 8.0°C, which was 0.8°C higher than in 2001. Thus, overall, the LST_{nt} increased over the period of the study.

Figure 4B shows the West (37.97 W) - East (76.55 East) profile of the annual LST_{nt} average from 2001 to 2020. Based on this profile, annual mean LST_{nt} values varied from -5.99 °C to 15.8°C across the profile line. Figure 4C shows the North (48.99 N) - South (26.05 S) annual profile, with LST_{nt} values varying from -3.0°C to 21.1°C. This profile clearly illustrates that the annual mean LST_{nt} values during the study period were higher in the southern half of the U.S., beginning at latitudes just below 40°N. The annual mean of 20-year LST_{nt} values map can thus be used as a predictor variable to examine the spatial relationships between the annual, mean LST_{nt} values and COPD mortality rates in the study area.

Figure 5 shows the average LST_{nt} difference from the beginning (2001) until the end (2020) of the study period based on the change of raster pixel (cell) values extracted from the MODIS images for those two years. As seen in Figure 5A, the change values varied from a minimum of about -12.5°C to a maximum of 8.9°C for specific places. In different counties, the mean changes varied from about -3.0°C to about 4.0°C. As demonstrated in Figure 5B, the changes in the eastern counties were higher than those in the western counties, with the LST_{nt} values in most counties of Missouri, Illinois, Indiana, New York, Florida and Mississippi showing increases. This indicates that these states had significant LST_{nt} changes throughout the 20 years under study. As seen in the map, the annual mean LST_{nt} change can also be used as another predictor variable to investigate the spatial relationships between annual mean LST_{nt} change values and COPD mortality rates as mentioned in the next section.

Relationships of LSTnt and the COPD mortality rates

Global spatial correlation

Before performing local correlation analysis, we tested the global spatial correlation between COPD mortality rates and study predictors by applying bivariate GMI to measure the spatial corre-

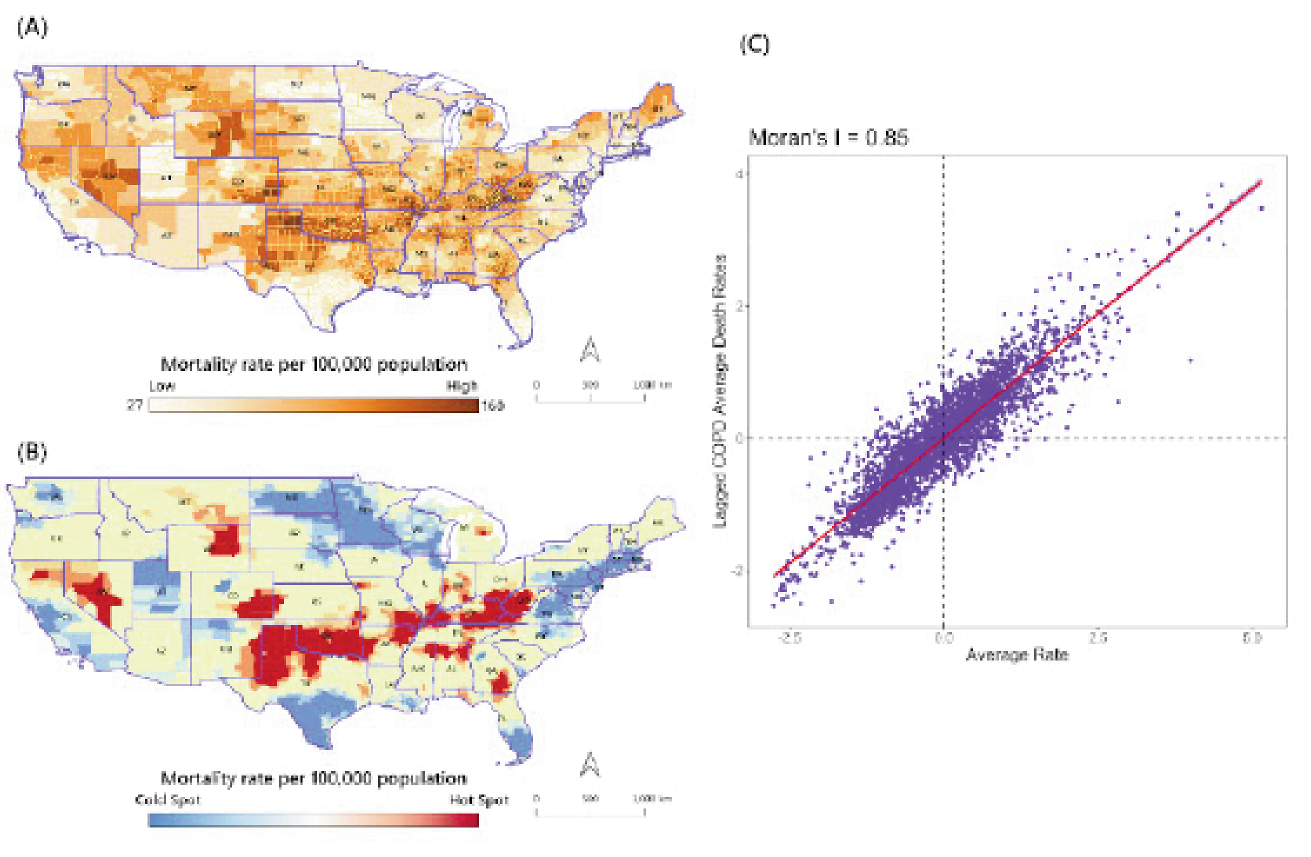

Figure 2. The 20-year-annual average COPD mortality rates per 100.000 population. (**A**) Spatial distribution map of rates across contiguous United States counties; (**B**) hotspots and coldspots of mortality rates calculated using Getis-Ord Gi* statistic; (**C**) the results of Global Moran's *I* scatter plots of the spatial autocorrelation.

lation between the average of COPD mortality rates and predictor variables (*i.e.*, LST_n mean and LST_{nt} change) for the study area resulting in $I = 0.18$, $p < 0.05$ and the z-score=22 with a confidence level of 95%. The null hypothesis was rejected because of the spatial correlation between COPD mortality rates and the 20-year mean of LST_{nt} values. These tests were also performed to measure the correlation between LST_{nt} change and the COPD mortality rates. We found that there was no spatial correlation between LST_{nt} change values and COPD mortality rates in the study area during this period. The LST_{nt} changes (rise and fall) were not associated with the COPD mortality rates. Given these findings, we performed a local analysis and developed a prediction model with the mean of LST_{nt} values and the COPD death rates as dependent and predictor parameters.

Local spatial correlation

Figure 6 shows the results of the exploration of the local spatial correlation of spatially lagged 20-year average of COPD mortality rates and the 20-year mean LST_{nt} in the study area. The intensity of the spatial correlation of the two variables was statistically significant in many counties, i.e., 366 counties with $p<0.001$ (99% CI), 426 counties with $p<0.01$ (95% CI) and 553 counties with $p<0.05$ (95% CI), so the null hypothesis was rejected (Figure 6A). The cluster map in Figure 6B represents the spatial correlation patterns of the two variables. In areas shaded in red, the values of the two variables were high in contrast to the areas shaded in blue, where they were low. In 19 states, (38.8% of the total), most counties were found to be in High-High clustered areas, e.g., Texas, Oklahoma, Arkansas, Kentucky, West Virginia, and Georgia. In contrast, Minnesota, Wisconsin and Utah were among states where most counties were located in Low-Low clusters.

Spatial prediction and model performance

Based on the annual mean of LST_{nt} an explanatory variable in this study, spatial prediction of the COPD mortality rates was attempted by applying the FCR model. With an R^2 of 0.78, a p-value less than 0.001, and a standard error approaching zero based on the model training diagnostics, the FCR model effectively explained the spatial predictions of COPD mortality in the study area. Figure 7A shows this based on natural breaks (Bajjali, 2023) and the choropleth approach. According to this prediction map and based on the twenty-year average of mortality rates and LST_{nt}, some counties should experience higher rates, e.g., counties in Kentucky, West Virginia, Maryland and Texas, which are among those most likely to move in this direction.

Figure 7B, shows the line chart of prediction intervals based on FCR model uncertainty parameters. The fields, ending with P05 (in green) and P95 (in blue), represent the upper and lower bounds of

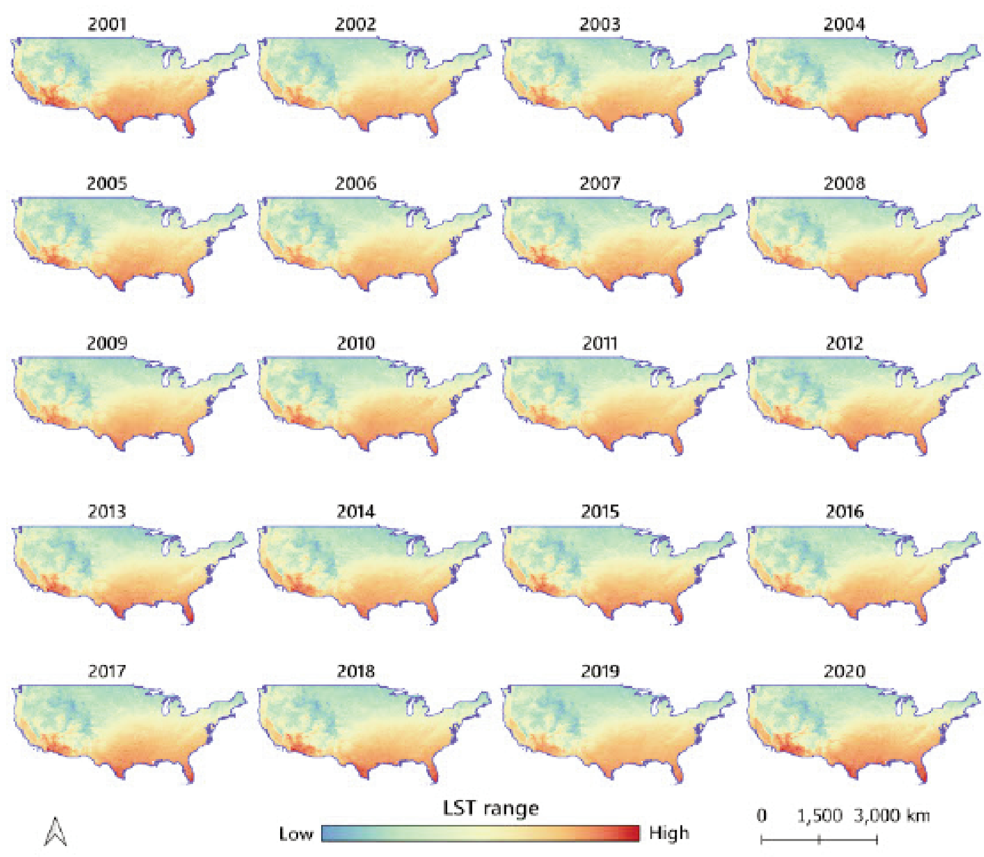

Figure 3. The spatial distribution maps of annual, mean LST_{nt} across contiguous United States for the years 2001 to 2020 based on MODIS data.

the prediction interval. For example, for Chaves County, New Mexico, the Federal Information Processing Standards code (FIPS) = 35005), the upper and lower bounds of the prediction interval are 100 and 86 per 100.000 population. For any new observation within this area, the value would be expected to fall with 90% confidence, given the same explanatory variables. Based on the FCR model, mortality rates were predicted to be higher than normal in more than 47% of counties (estimated mean = 74).

The FCR model must be calibrated and validated to accurately predict rates. Bivariate map and scatter plot were used for model calibration and validation of predicted rates (as described in the model validation section). The bivariate map was used to quantify the degree of spatial agreement between two continuous valued fields (“predicted rates” and “original rates”) in a single map. Figure 8A shows the spatial distribution bivariate maps of the local spatially varying predicted rates and the original rate values, which are aggregated at the county scale. This bivariate map shows that there is strong agreement between original and predicted rates. Areas shaded in dark brown are counties where COPD mortality “original rates” and “predicted rates” match. Using the scatterplot, the goodness of fit between FCR model predictions and reality was validated in the study area based on FCR model diagnostics. The model accurately predicted 68% of the relationship with an R^2 value of 0.68 (Figure 8 B).

Discussion

According to our findings, the spatial distribution of COPD mortality rates in the contiguous U.S. was not distributed homogeneously. We identified significant hotspot counties where rates were clustered, a spatial heterogeneity with respect to COPD mortality rates that was confirmed at the 0.85 level by Moran’s *I*. Presumably, various risk factors may have contributed to this geographic clustering, notably, counties in southern states, such as Kentucky, West Virginia and Oklahoma, all of which ranked high with regard to COPD mortality. These counties have also been identified in previous studies (Dwyer-Lindgren *et al.*, 2014; Liu *et al.,* 2020) as having high smoking prevalence rates. A CDC report (2020) covering 2016 to 2020 showed that these counties were among those with high rates of lung and bronchial cancer (>40 per 100.000 people). However, according to Liu *et al.* (2020) note that these counties also have high amounts of air pollutants including $PM_{2.5}$, while the National Institutes on Minority Health and Health Disparities (NIMHD) refers to other papers reporting high poverty rates, (NIMHD, 2023) and CDC (2023) reports high rates of asthma prevalence among adults in these same areas, so the problem is clearly multifactorial. We found that mortality rates were higher in most urbanized areas. According to Bounoua *et al.* (2017), urbanization added an annual warming of 1.1C^{o}. Increases in urban sur-

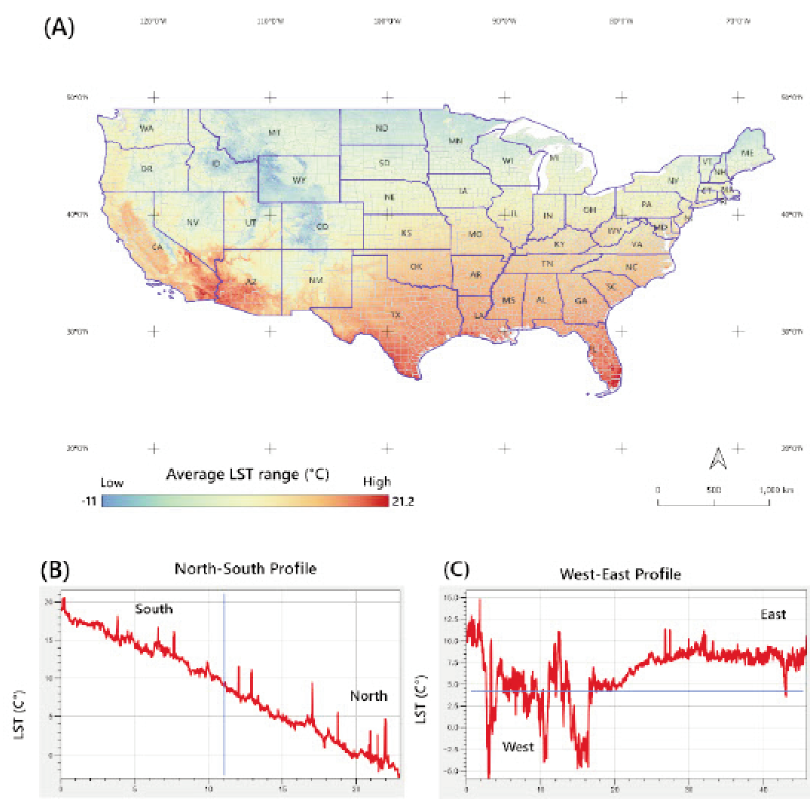

Figure 4. The spatial distribution of LST_{nt} average values in the contiguous U.S. (**A**) Low to high range values of the annual mean LST_{nt} based on MODIS 1.2 km-resolution images; (**B**) North to South profile line of annual mean LST_{nt} values; (**C**) West to East profile line of annual mean LST_{nt} values.

face temperature lead to higher frequency and severity of heat waves in most urbanized areas and cities, and this must also affect the population's health. The Health Equity Report from the Department of Health and Human Services, Health Resources and Services Administration (2020) shows high poverty rates in some states e.g., Kentucky and Georgia, which we identified as areas with high COPD mortality rates. The findings on the spatial distribution of COPD mortality rates reveal significant geographic disparities, particularly in southern states like Kentucky, West Virginia, and Oklahoma, where rates are clustered. This underscores the multifactorial nature of COPD. In addition to other significant risk factors for COPD mortality, several should be considered, including genetic predisposition, occupational exposures to harmful substances, chronic respiratory infections, limited access to healthcare, poor nutritional status, mental health conditions, passive smoking, broader socioeconomic factors (American Lung Association, 2024), Climate Change, and urban planning.

This study focused primarily on the relationship between LST and COPD mortality. However, other significant risk factors for COPD, including smoking and pollution, were not included in the analysis. These factors are known to play a critical role in COPD outcomes, and their exclusion may limit the interpretation of the results reported here. For example, we compared maps from the U.S. Census Bureau and the Behavioral Risk Factor Surveillance System (BRFSS) (Ney, 2023; Wu *et al.*, 2020) highlighting areas with high air pollution or smoking rates to the map displaying higher COPD mortality rates. We found that many areas with high air pollution or elevated smoking rates exhibit similar patterns to those with high COPD mortality. This suggests that areas with high air pollution or smoking rates may experience elevated COPD mortality rates irrespective of the LST patterns.

Addressing these diverse factors can lead to a more comprehensive understanding of COPD risk and inform targeted public health interventions. These insights highlight the need for targeted public health interventions and policies in high-risk areas, promoting smoking cessation, improving air quality, and addressing health disparities. Additionally, the study emphasizes the importance of considering local context in health strategies and opens avenues for further research into the mechanisms behind the observed clustering, ultimately enhancing understanding and informing future public health initiatives.

The increased average, annual LST_{nt} values found by our study over the 2001-2020 period are in line with the National Centers for Environmental Information report (NIMHD, 2023), which has confirmed that the mean surface air temperature in the contiguous U.S. increased at an average rate of 0.17°F (0.09°C) per decade. Accelerated urbanization and urban sprawl are significant components of land cover, land use and local climate change in the U.S.

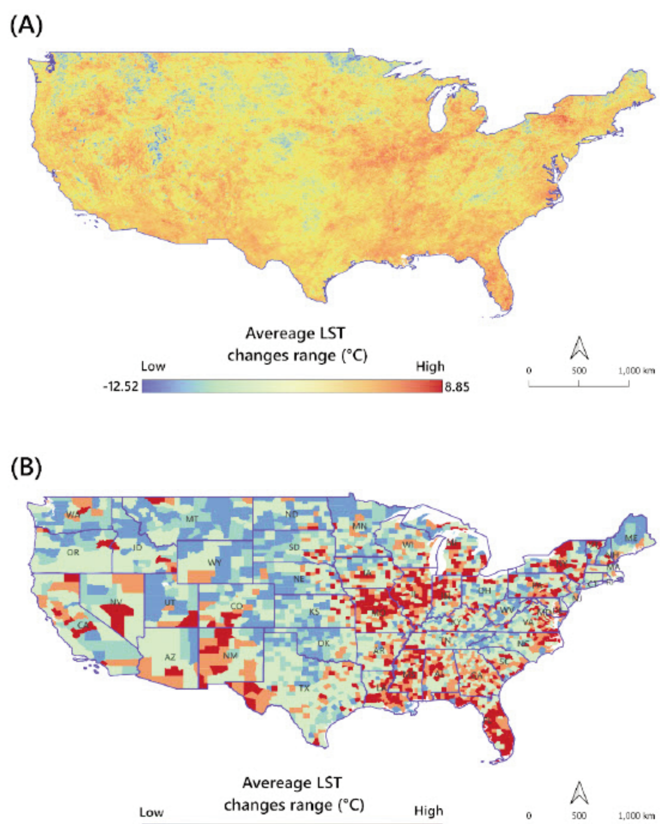

Figure 5. The spatial distribution of annual, mean LST_{nt} change values with difference between 2001 and 2020 as start and end dates in contiguous United States counties. (**A**) Annual mean LSTnt values from low to high values; (**B**) annual mean LSTnt change values collected for the counties.

(Bounoua *et al.*, 2018). Therefore, presumably, human-caused environmental changes and activities in the form of construction and new developments are among the most crucial drivers of the LST_{nt} increase noted in our study.

Built-up areas are well-known for having higher temperatures than their rural surroundings and this urban heat island effect has been observed to raise the LST_{nt} of cities by about 2.0 to 5.0°F (1.0 to 3.0°C) (NASA, 2023). Counties identified as areas with the highest LST_{nt} changes in this study, are also those where peri-urban and urban expansion have taken place according to the Global Human Settlement Layer (GHSL) study (Kemper *et al.*, 2017). The rise of LST_{nt} is due to the presence of asphalt, concrete, stone, steel and other surfaces that absorb heat and disrupt the natural cooling effect provided by vegetation (Bounoua *et al.*, 2015). Human activities have also led to loss of land cover, changes in land morphology, fires and deforestation, e.g., in U.S. counties with high rates of LST_{nt}, 7.2% of the tree cover was lost from 2001 to 2022 (Zanin & Sillère, 2015). According to the same report, deforestation and wildfire incidents directly contributed to the rise in environmental contaminants and the deterioration of respiratory diseases. Our results confirm that the nationwide mean of high COPD mortality rates and the increasing annual mean LST_{nt} are positively associated. In addition, the highly significant local spatial correlation in 38% of all counties emphasize the important role of temperature in this scenario, a finding consistent with various studies indicating that rising temperatures are accompanied by increasing COPD mortality rates (Almetwally *et al.*, 2020; Tian *et al.*, 2021; Fu *et al.*, 2022; Gu *et al.*, 2022). Indeed, increasing temperature at night, increases the mortality rates among people with respiratory diseases. Thus, ambient heat during the night may interrupt the normal physiology of sleep. Less sleep can then lead to an ineffective immune system and a higher risk of both acute and chronic illnesses (He *et al.*, 2022).

The absence of significant correlation between LST_{nt} change rates and COPD mortality rates was an unexpected finding. This could be due to new construction or urban growth in general (Levitt & Eng, 2021), which is known to increase LST_{nt} levels. Another reason is that most counties characterized by changes in LST_{nt} are located in areas undergoing land cover changes, such as deforestation with large-scale impact on vegetation as reported in the last 20 years (Global Forest Watch, 2023). While low COPD mortality rates were seen during the study period in newly constructed areas with low population density and impervious surface areas, counties with high LST_{nt} changes and built-up area growth rates may be considered as likely places in the future to record health problems, including COPD.

The study presents several novel findings related to COPD mortality rates, particularly by identifying significant hotspot counties with clustered mortality rates. It highlights an average increase in annual land surface temperature (LSTnt) from 2001 to 2020, emphasizing the importance of local temperature changes. Additionally, a positive correlation was established between rising

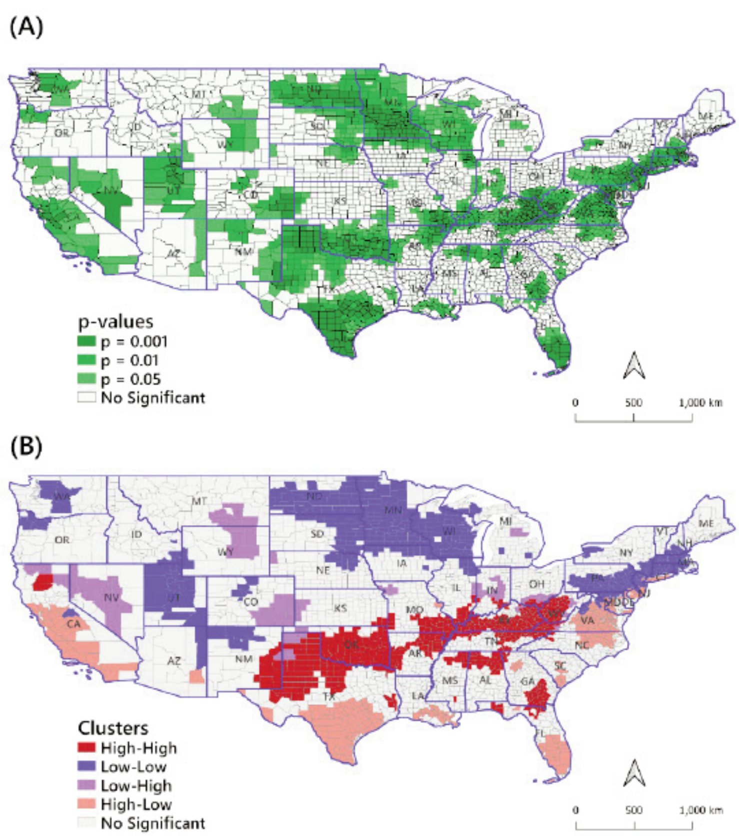

Figure 6. Spatial correlation between COPD mortality rates and annual mean LSTnt across the contiguous United States. (**A**) P-values (**B**) Clusters.

temperatures and COPD mortality rates, aligning with existing research while offering county-level insights into climate change as a contributing risk factor for respiratory diseases. These findings enhance the understanding of the spatial distribution of COPD mortality and underscore the need for targeted public health interventions in high-risk areas.

Limitations and future research directions

In spite of strengths, such as the identification of COPD mortality hotspots across U.S. counties based on LST_{nt} trends and changes over 20 years, extracted by remote sensing, for which a validated FCR model was used to predict precise estimates of COPD mortality rates, some limitations must be acknowledged. This study primarily examined the spatial correlation between LST and COPD mortality rates. However, incorporating other critical risk factors—such as air pollutants, smoking rates, vegetation, land cover changes, and environmental hazards (*e.g.*, floods and fires)—as control variables would offer a more comprehensive understanding of how climate change impacts COPD mortality. The absence of these control variables in the current analysis means that the true effect of climate change on COPD mortality may not be fully captured. Including these factors could potentially modify the relationship between LST and COPD mortality.

Second, we used remotely sensed data for correlation measurement. The use of synoptic and real-data aggregated from weather stations may show different results that we did not address. Finally, the FCR model that has been used in this study was providing suitable results. However, it does not consider the long and defined time period for future predictions and uses previous or present space-time evidence. In future studies, models that consider long-time predilections should be used. However, access to projected or modelled LST_{nt} values for certain periods must be assured. Further, climate changes can create very complex environmental effects from different dimensions, which are necessary to investigate to face their possible risks for public health. In future research, information on environmental factors, such as land cover change, air pollutants and environmental hazards, should be taken into account in detailed spatial relationships and predictions to better inform our understanding of climate and environmental changes to public health as well as respiratory diseases. Based on the findings of this research, we present some strategies to reduce the vulnerability caused by climate change. These predictions should help local public health authorities in planning and allocating resources with a focus on the counties at the highest risk.

Policy implications

Reducing or preventing vulnerability caused by climate change requires the use of integrated solutions (Lin *et al.*, 2021). The findings regarding COPD mortality rates and their connection to factors, such as land surface temperature highlight the urgent need for integrated strategies to reduce vulnerabilities related to climate change. Key implementations should involve long-term initiatives

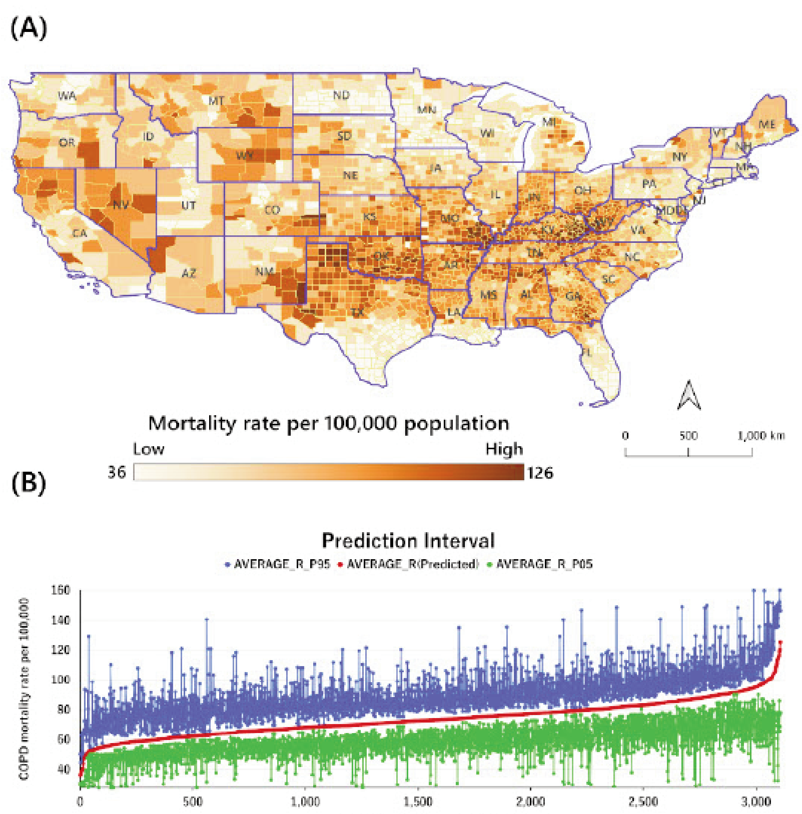

Figure 7. Prediction map of the COPD mortality rates based on the annual mean LST_{nt}. (**A**) Spatial distribution of mortality rates by county; (**B**) Prediction interval chart of predicted rates. Note: Blue bars indicate higher than the predicted average values and green bars lower than these values.

focused on preventing deforestation and promoting reforestation, alongside the incorporation of nature-based solutions like green roofs and urban gardens to bolster urban resilience. Integrating green technologies into urban planning can significantly mitigate heat islands and enhance air quality. Furthermore, aligning these environmental strategies with social welfare and healthcare programs is essential to provide comprehensive support for at-risk communities. Effective collaboration among stakeholders, including local governments, health organizations, and community groups, will be crucial in addressing the multifaceted challenges posed by climate change, ultimately improving respiratory health outcomes for vulnerable populations. Engaging with local communities in these initiatives ensures that strategies are tailored to specific needs and contexts, thereby enhancing their effectiveness and sustainability.

Conclusion

This study predicted COPD mortality rates based on historical mean LST_{nt} trends across U.S. counties. With an R^2 of 0.78, the FCR model accurately explained spatial predictions of COPD mortality based on the annual mean of LST_{nt} and the model used in this study predicted the likelihood of COPD mortality rates. However, the severity of this association varied spatially and some counties were more effected than others. Furthermore, areas with severe recent LST_{nt} changes did not necessarily have high mortality rates. As a result, recent LST_{nt} and environmental changes may have a delayed, long-term impact on COPD patients. This study findings could help people in charge of health and spatial policy to establish long-term policies and plans for lowering vulnerability to climate change.

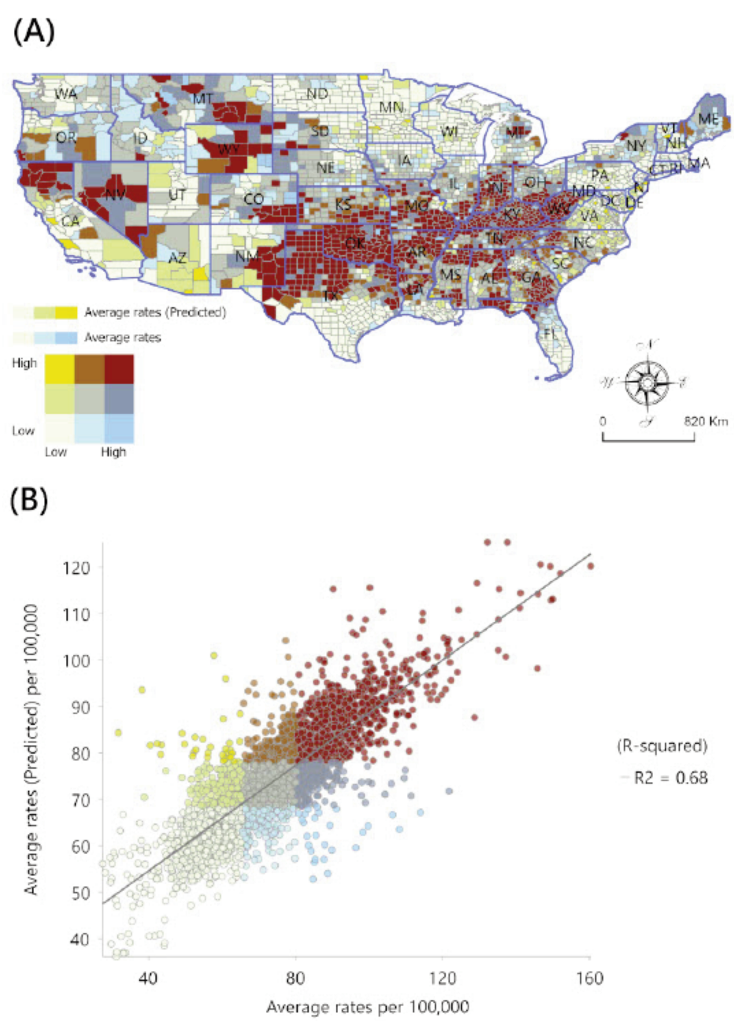

Figure 8. Correlation between the original and predicted values of the COPD mortality rates of United States counties based on the FCR model. (**A**) Spatial distribution bivariate map of original and predicted values; (**B**) Scatterplot measures the goodness of the fit of FCR model results.

References

Addis A, 2023. GIS–based flood susceptibility mapping using frequency ratio and information value models in upper Abay River basin, Ethiopia. Nat Hazards Res 3:247-56.

Almetwally AA, Bin-Jumah M, Allam AA, 2020. Ambient air pollution and its influence on human health and welfare: an overview. Environ Sci Pollut Res Int 27:24815–30.

Alvarez-Mendoza CI, Teodoro A, Freitas A, Fonseca J, 2020. Spatial estimation of chronic respiratory diseases based on machine learning procedures—an approach using remote sensing data and environmental variables in Quito, Ecuador. Appl Geogr 123:102273.

American Lung Association, 2023. COPD trends brief: mortality. Retrieved June 16, 2023. Available from: https://www.lung.org/research/trends-in-lung-disease/copd-trends-brief/copd-mortality

American Lung Association, 2024. What causes COPD? Retrieved October 10, 2024. Available from: https://www.lung.org/lung-health-diseases/lung-disease-lookup/copd

Anselin L, 2020. Local Spatial Autocorrelation. Other Local Spatial Autocorrelation Statistics.

Anselin L, Syabri I, Kho Y, 2009. GeoDa: an introduction to spatial data analysis. In: Handbook of applied spatial analysis: software tools, methods and applications, Springer, pp. 73-89.

Bajjali W, 2023. Introduction to ArcGIS Pro. In: ArcGIS Pro and ArcGIS Online: applications in water and environmental sciences, Springer, pp. 1-14.

Bala R, Prasad R, Yadav VP, 2020. A comparative analysis of day and night land surface temperature in two semi-arid cities using satellite images sampled in different seasons. Adv Space Res 66:412-25.

Bounoua L, Nigro J, Zhang P, Thome K, Lachir A, 2018. Mapping urbanization in the United States from 2001 to 2011. Appl Geogr 90:123-33.

Bounoua L, Zhang P, Mostovoy G, Thome K, Masek J, Imhoff M, Shepherd M, Quattrochi D, Santanello J, Silva J, 2015. Impact of urbanization on US surface climate. Environ Res Lett 10:84010.

Bounoua L, Zhang P, Nigro J, Lachir A, Thome K, 2017. Regional impacts of urbanization in the United States. Can J Remote Sens 43:256-68.

Bracke KR, Brusselle GG, 2015. Chapter 97 - Chronic obstructive pulmonary disease. In: Mestecky J, Strober W, Russell MW, Kelsall BL, Cheroutre H, Lambrecht BN, eds. Immunology, Fourth ed. Boston: Academic Press, pp. 1857-66.

Breiman L, Cutler A, 2001. Random forests. Mach Learn 45:5-32.

Celli B, Fabbri L, Criner G, Martinez FJ, Mannino D, Vogelmeier C, Montes de Oca M, Papi A, Sin DD, Han MK, Agusti A, 2022. Definition and nomenclature of chronic obstructive pulmonary disease: time for its revision. Am J Respir Crit Care Med 206:1317-25.

Center for Sustainable Systems, University of Michigan, 2019. US cities factsheet. Report No. CSS09-06.

Centers for Disease Control and Prevention (CDCP), 2020. Cancer statistics at a glance: rate of lung and bronchus cancer deaths in the United States, 2016-2020. Retrieved August 3, 2024. Available from: https://gis.cdc.gov/Cancer/USCS/#/AtAGlance/

Centers for Disease Control and Prevention (CDCP), 2023. COPD. Retrieved June 16, 2023. Available from: https://www.cdc.gov/dotw/copd/index.html

Chen J, Shi C, Li Y, Ni H, Zeng J, Lu R, Zhang L, 2021. Effects of short-term exposure to ambient airborne pollutants on COPD-related mortality among the elderly residents of Chengdu City in Southwest China. Environ Health Prev Med 26:7.

Chuang H, Huan MT, Chen T, Lu Y, Chen K, Ho S, Wu C, Lee K, 2022. Climate change and COPD severity: a pilot study in Taiwan. Eur Respir J 60:1998.

Cushen B, Morgan R, Summer R, 2017. Chronic obstructive pulmonary disease. In: Quah S, ed. Oxford: Academic Press, pp. 28-35.

D'Amato G, Cecchi L, D'Amato M, Annesi-Maesano I, 2014. Climate change and respiratory diseases. Eur Respir Rev 23:161-9.

de Miguel-Díez J, Hernández-Vázquez J, López-de-Andrés A, Álvaro-Meca A, Hernández-Barrera V, Jiménez-García R, 2019. Analysis of environmental risk factors for chronic obstructive pulmonary disease exacerbation: A case-crossover study (2004-2013). PLoS One 14:e0217143.

Di Mari R, Ingrassia S, Punzo A, 2023. Local and overall deviance R-squared measures for mixtures of generalized linear models. J Classif 2023:1-34.

Diao LJ, Gao ZH, Jiang YC, Chen ZS, Li N, Meng XF, Xu X, Li J, 2021. Linear and interactive effects of air pollution and diurnal temperature range on COPD mortality in Weifang, China: a time series analysis. Biomed Environ Sci 34:662-6.

Donaldson, Gavin C., James J. Goldring, and Jadwiga A. Wedzicha. 2012. Influence of season on exacerbation characteristics in patients with COPD. Chest 141:94-100.

Duan R-R, Hao K, Yang T, 2020. Air pollution and chronic obstructive pulmonary disease. Chronic Dis Transl Med 6:260-9.

Duvat VK E, Magnan AK, Perry CT, Spencer T, Bell JD, Wabnitz CC C, Webb AP, White I, McInnes KL, Gattuso J-P, 2021. Risks to future atoll habitability from climate-driven environmental changes. Wiley Interdiscip Rev Clim Change 12:e700.

Dwyer-Lindgren L, Mokdad AH, Srebotnjak T, Flaxman AD, Hansen GM, Murray CJL, 2014. Cigarette smoking prevalence in US counties: 1996-2012. Popul Health Metrics 12:5.

Environmental Systems Research Institute (ESRI), 2010. ArcGIS professional GIS help. Retrieved August 4, 2024, from https://pro.arcgis.com/en/pro-app/latest/help.

Friedman JH, 2001. Greedy function approximation: a gradient boosting machine. Ann Stat 29:1189-232.

Fu S, Zhou Y, Peng L, Ye X, Yang D, Yang S, Zhou J, Luo B, 2022. Interactive effects of high temperature and ozone on COPD deaths in Shanghai. Atmos Environ 278:119092.

Geodatos, 2023. United States geographic coordinates. Retrieved March 1, 2024. Available from: https://www.geodatos.net/en/coordinates/united-states.

Global Forest Watch, 2023. Global Forest Watch. Retrieved April 1, 2024. Available from: https://www.globalforestwatch.org/dashboards/country/USA.

Griffith DA, 2009. Modeling spatial autocorrelation in spatial interaction data: empirical evidence from 2002 Germany journey-to-work flows. J Geogr Syst 11:117–40.

Gu S, Wang X, Mao G, Huang X, Wang Y, Xu P, Wu L, Lou X, Chen Z, Mo Z, 2022. The effects of temperature variability on mortality in patients with chronic obstructive pulmonary disease: a time-series analysis in Hangzhou, China. Environ Sci Pollut Res 29:71502–10.

Hansel NN, McCormack MC, Kim V, 2016. The effects of air pollution and temperature on COPD. COPD 13:372–9.

He C, Kim H, Hashizume M, Lee W, Honda Y, Kim SE, Kinney PL, Schneider A, Zhang Y, Zhu Y, Zhou L, Chen R, Kan H, 2022. The effects of night-time warming on mortality burden under future climate change scenarios: a modelling study. Lancet Planet Health 6:e648-57.

Hess JJ, Heilpern KL, Davis TE, Frumkin H, 2009. Climate change and emergency medicine: impacts and opportunities. Acad Emerg Med 16:782-94.

Hurst JR, Skolnik N, Hansen GJ, Anzueto A, Donaldson GC, Dransfield MT, Varghese P, 2020. Understanding the impact of chronic obstructive pulmonary disease exacerbations on patient health and quality of life. Eur J Intern Med 73:1-6.

Jenkins CR, Celli B, Anderson JA, Ferguson GT, Jones PW, Vestbo J, Yates JC, Calverley PMA, 2012. Seasonality and determinants of moderate and severe COPD exacerbations in the TORCH study. Eur Respir J 39:38-45.

Joshi MY, Aliaga DG, Teller J, 2023. Predicting urban heat island mitigation with random forest regression in Belgian cities. Pp. 305-23 in International Conference on Computers in Urban Planning and Urban Management. Springer.

Kemper T, Corban C, Ehrlich D, Florczyk A, Freire SMC, Maffenini L, Melchiorri M, Politis P, Schiavina M, Pesaresi M, 2017. GHS built-up grid, derived from Landsat, multitemporal (1975, 1990, 2000, 2014), IR2017 V1. 0.

Levitt Z, Eng J, 2021. Where America's developed areas are growing: 'Way off into the horizon.' The Washington Post, August 11. Accessed: 1 January 2024. Available from: https://www.washingtonpost.com/nation/interactive/2021/land-development-urban-growth-maps/

Li J, 2019. A critical review of spatial predictive modeling process in environmental sciences with reproducible examples in R. Appl Sci 9:2048.

Lin BB, Ossola A, Alberti M, Andersson E, Bai X, Dobbs C, Elmqvist T, Evans KL, Frantzeskaki N, Fuller RA, Gaston KJ, Haase D, Jim CY, Konijnendijk C, Nagendra H, Niemelä J, McPhearson T, Moomaw WR, Parnell S, Pataki D, Ripple WJ, Tan PY, 2021. Integrating solutions to adapt cities for climate change. Lancet Planet Health 5:e479-86.

Liu B, Sze J, Li L, Ornstein KA, Taioli E, 2020. Bivariate spatial pattern between smoking prevalence and lung cancer screening in US counties. Int J Environ Res Public Health 17:3383.

Livings M, Wu A M, 2020. Local measures of spatial association. In: Wilson J P, editor. The Geographic Information Science & Technology Body of Knowledge. University Consortium for Geographic Information Science.

Lovejoy S, 2013. What is climate? Retrieved January 5, 2023. Available from: https://agupubs.onlinelibrary.wiley.com/doi/10.1002/2013EO010001Di

Martínez M G, Pérez-Castro E, Reyes-Carreto R, Acosta-Pech R, 2022. Spatial modeling in epidemiology. In: Vargas-De-León C, editor. Rijeka: IntechOpen.

McCormack MC, Paulin LM, Gummerson CE, Peng RD, Diette GB, Hansel NN, 2017. Colder temperature is associated with increased COPD morbidity. Eur Respiratory J 49:1601501.

Mertes H, Schoierer J, Gutknecht T, Hieronimi A, Mambrey V, Schmidt I, Böse-O'Reilly S, Lob-Corzilius T, 2021. Climate change and health. Internistische Praxis 64:533-44.

NASA LP DAAC, 2023. MOD11A2 V061 MODIS/Terra land surface temperature/emissivity 8-day L3 global 1 km SIN grid. Retrieved March 1, 2024. Available from: https://lpdaac.usgs.gov/products/mod11a2v061/

NASA, 2023. Vegetation limits city warming effects. Retrieved January 1, 2024. Available from: https://earthobservatory.nasa.gov/images/86440/vegetation-limits-city-warming-effects

National Centers for Environmental Information, 2023. Climate at a glance national time series. Available from: ADD LINK

National Institutes on Minority Health and Health Disparities (NIMHD), 2023. Poverty for United States by county 2017-2021.

Ney J. 2023. Map: American Inequality. Created with Datawrapper. Retrieved November 21, 2024. Available from: https://www.datawrapper.de/_/f0xhf/

Ozturk Y, Baltaci H, Akkoyunlu BO, 2023. The effects of heat-waves on hospital admissions in the Edirne Province of Turkey: A cohort study. Medicine 102:e34299.

Peng Q, Zhang N, Yu H, Shao Y, Ji Y, Jin Y, Zhong P, Zhang Y, Jiang H, Li C, Shi Y, Zheng Y, Xiong Y, Wang Z, Jiang F, Chen Y, Jiang Q, Zhou Y, 2021. Geographical variation of COPD mortality and related risk factors in Jiading District, Shanghai. Front Public Health 9:627312.

Phillips S J, Dudík M, 2008. Modeling of species distributions with Maxent: New extensions and a comprehensive evaluation. Ecography 31:161-75.

QGIS Development Team, 2016. QGIS geographic information system. Open-Source Geospatial Foundation Project.

Rasul A, Balzter H, Smith C, 2016. Diurnal and seasonal variation of surface urban cool and heat islands in the semi-arid city of Erbil, Iraq. Climate 4:42.

Sama SR, Kriebel D, Gore RJ, DeVries R, Rosiello R, 2017. Environmental Triggers of COPD Symptoms: A Case Cross-over Study. BMJ Open Respir Res 4:e000179.

Shiau, Yuo Hsien, Su Fen Yang, Rishan Adha, Syamsiyatul Muzayyanah, and Giia Sheun Peng. 2023. The Exposure-Response of Air Pollution and Climate Change to Chronic Respiratory Diseases: Does Residential Energy Efficiency Matter? Urban Climate 51:101649.

Subramanian A, Mosur Nagarajan A, Vinod S, Chakraborty S, Sivagami K, Theodore T, Sathyanarayanan S S, Tamizhdurai P, Mangesh V L, 2023. Long-term impacts of climate change on coastal and transitional eco-systems in India: An overview of its current status, future projections, solutions, and policies. RSC Advances 13:12204-28.

Tian H, Zhou Y, Wang Z, Huang X, Ge E, Wu S, Wang P, Tong X, Ran P, Luo M, 2021. Effects of high-frequency temperature variabilities on the morbidity of chronic obstructive pulmonary disease: Evidence in 21 cities of Guangdong, South China. Environ Res 201:111544.

Tilstra M H, Nielsen C C, Tiwari I, Jones C A, Osornio Vargas A, Quemerais B, Bulut O, Salma J, Yamamoto S S, 2022. Exploring socio-environmental effects on community health in Edmonton, Canada to understand older adult and immigrant risk in a changing climate. Urban Climate 44:101225.

Tourre Y M, Paulin M, Gilles D, Attias D, Pathak A, 2022. COVID-19, air quality and space monitoring. Geospatial Health 17:1052.

Tran H M, Chuang T W T W, Chuang H C H, Tsai F J F, 2023. Climate change and mortality rates of COPD and asthma: A global analysis from 2000 to 2018. Environ Res 116448:116448.

Tran H M, Tzu-Tao Chen T T, Yueh-Hsun Lu Y H, Tsai F J F, Kuan-Yuan Chen K Y, Ho S C, Wu C D, Wu S M, Wu Y L, Lee Y L, Chung K F, Kuo H P, Kang-Yun Lee K Y, Chuang H C, 2022. Climate-mediated air pollution associated with COPD severity. Sci Total Environ 843:156969.

United States Census Bureau, 2022. County Population by Characteristics: 2010-2022 Accessed: 3 January 2024. Available from: https://www.census.gov/data/datasets/time-series/demo/popest/2010s-counties-detail.html

United States Department of Health and Human Services, Health Resources and Services Administration, Office of Health Equity (2020) Health Equity Report 2019-2020: Special Feature on Housing and Health Inequalities. Rockville, Maryland: Health Resources and Services Administration. Accessed: 1 January 2024. Available from: https://www.hrsa.gov/sites/default/files/hrsa/about/news/hrsa-health-equity-report.pdf

Viggers H, Howden-Chapman P, Ingham T, Chapman R, Pene G, Davies C, Currie A, Pierse N, Wilson H, Zhang J, 2013. Warm homes for older people: Aims and methods of a randomised community-based trial for people with COPD. BMC Public Health 13:1-12.

Wan Z, Hook S, Hulley G, 2021. MODIS/Terra land surface temperature/emissivity monthly L3 global 0.05Deg CMG V061 [Data Set]. NASA EOSDIS Land Processes Distributed Active Archive Center 61.

Wang J, Wu Y, Hsu H-H, Cheng Z, 2017. Chapter 7 - Spatial big data analytics for cellular communication systems. Pp. 153-66 in Intelligent Data-Centric Systems, edited by H-H Hsu and C-Y Chang. Academic Press.

World Health Organization (WHO), 2023a. Ambient air pollution. Retrieved March 16, 2023 https://www.who.int/data/gho/data.

World Health Organization (WHO), 2023b. Chronic obstructive pulmonary disease (COPD). Retrieved February 2, 2023. Available from: https://www.who.int/news-room/fact-sheets/detail/chronic-obstructive-pulmonary-disease-(copd).

Htwe ZC, Laohasiriwong W, Sornlorm K, Mahato R, 2023. Spatial pattern and heterogeneity of chronic respiratory diseases and relationship to socio-demographic factors in Thailand in the period 2016 to 2019. Geospat Health 18:1203.

Wu X, Nethery RC, Sabath MB, Braun D, Dominici F, 2020. Air Pollution and COVID-19 Mortality in the United States: Strengths and Limitations of an Ecological Regression Analysis. Sci Adv 6:eabd4049.

Zafirah Y, Lin Y-K, Andhikaputra G, Deng L-W, Sung F-C, Wang Y-C, 2021. Mortality and morbidity of asthma and chronic obstructive pulmonary disease associated with ambient environment in metropolitans in Taiwan. Plos One 16:e0253814.

Zanin C, Sillère G, 2015. Global forest watch, Mappemonde, 114(2), p. 1. Accessed: 1 April 2024. Available at: https://www.globalforestwatch.org/dashboards/country/USA